

Effects of heterogeneous adoption thresholds on contact-limited social contagions

Dan-Dan Zhao(赵丹丹), Wang-Xin Peng(彭王鑫), Hao Peng(彭浩), and Wei Wang(王伟)
Citation: Chin. Phys. B, 2022, 31 (**6**): 068906. DOI: 10.1088/1674-1056/ac4e04
Journal homepage: http://cpb.iphy.ac.cn; http://iopscience.iop.org/cpb

What follows is a list of articles you may be interested in

A novel similarity measure for mining missing links in long-path networks

Yijun Ran(冉义军), Tianyu Liu(刘天宇), Tao Jia(贾韬), and Xiao-Ke Xu(许小可)
Chin. Phys. B, 2022, 31 (**6**): 068902. DOI: 10.1088/1674-1056/ac4483

Cascading failures of overload behaviors using a new coupled network model between edges

Yu-Wei Yan(严玉为), Yuan Jiang(蒋沅), Rong-Bin Yu(余荣斌), Song-Qing Yang(杨松青), and Cheng Hong(洪成)
Chin. Phys. B, 2022, 31 (**1**): 018901. DOI: 10.1088/1674-1056/ac1337

Evolution mechanism of Weibo top news competition

Fuzhong Nian(年福忠), Jingzhou Li(李经洲), and Xin Guo(郭鑫)
Chin. Phys. B, 2021, 30 (**12**): 128901. DOI: 10.1088/1674-1056/ac05ac

Contagion dynamics on adaptive multiplex networks with awareness-dependent rewiring

Xiao-Long Peng(彭小龙) and Yi-Dan Zhang(张译丹)
Chin. Phys. B, 2021, 30 (**5**): 058901. DOI: 10.1088/1674-1056/abe1ab

Exploring individuals' effective preventive measures against epidemics through reinforcement learning

Ya-Peng Cui(崔亚鹏), Shun-Jiang Ni (倪顺江), and Shi-Fei Shen(申世飞)
Chin. Phys. B, 2021, 30 (**4**): 048901. DOI: 10.1088/1674-1056/abcfa5

Effects of heterogeneous adoption thresholds on contact-limited social contagions

Dan-Dan Zhao(赵丹丹)[1], Wang-Xin Peng(彭王鑫)[2], Hao Peng(彭浩)[1,3], and Wei Wang(王伟)[4,†]

[1] *College of Mathematics and Computer Science, Zhejiang Normal University, Jinhua* 321004, *China*
[2] *College of Information, Zhejiang Guangsha Vocational and Technical University of Construction, Dongyang* 322100, *China*
[3] *Shanghai Key Laboratory of Integrated Administration Technologies for Information Security, Shanghai* 200240, *China*
[4] *School of Public Health and Management, Chongqing Medical University, Chongqing* 400016, *China*

(Received 6 October 2021; revised manuscript received 29 December 2021; accepted manuscript online 24 January 2022)

Limited contact capacity and heterogeneous adoption thresholds have been proven to be two essential characteristics of individuals in natural complex social systems, and their impacts on social contagions exhibit complex nature. With this in mind, a heterogeneous contact-limited threshold model is proposed, which adopts one of four threshold distributions, namely Gaussian distribution, log-normal distribution, exponential distribution and power-law distribution. The heterogeneous edge-based compartmental theory is developed for theoretical analysis, and the calculation methods of the final adoption size and outbreak threshold are given theoretically. Many numerical simulations are performed on the Erdös–Rényi and scale-free networks to study the impact of different forms of the threshold distribution on hierarchical spreading process, the final adoption size, the outbreak threshold and the phase transition in contact-limited propagation networks. We find that the spreading process of social contagions is divided into three distinct stages. Moreover, different threshold distributions cause different spreading processes, especially for some threshold distributions, there is a change from a discontinuous first-order phase transition to a continuous second-order phase transition. Further, we find that changing the standard deviation of different threshold distributions will cause the final adoption size and outbreak threshold to change, and finally tend to be stable with the increase of standard deviation.

Keywords: social contagions, threshold distribution, heterogeneous adoption thresholds, limited contact

PACS: 89.75.Hc, 87.19.X–, 87.23.Ge **DOI:** 10.1088/1674-1056/ac4e04

1. Introduction

Complex networks are embodied in fields of nature, society, science and technology.[1–9] A real complex system can be abstracted as a network, and then complex properties of the system, such as structure, robustness, function, as well as dynamical processes that occur on networks, can be investigated.[10–23] According to different characteristics of spreading objects, the spreading dynamics on complex networks can be generally divided into two categories: one is the dynamics of biological contagions with independent infection probabilities of any two contacts, such as the epidemic spreading and the spreading of computer viruses,[24–30] the other is the dynamics of social contagions with social reinforcement effect, including rumor diffusion, information spreading, behavior spreading, innovation adoption, and so on.[31–38] It is generally believed that social contagion is the expansion and application of biological contagion, and it is the research basis of social-biological coupling contagion.[39–43]

For the convenience of description, what is transmitted in social contagions is called "behavior", and behavior spreading is an essential form of social contagions. The social reinforcement effect described in the classic linear threshold model is memoryless, where the adoption threshold is the number or proportion of neighbors in the adopted state.[44,45] Considering the non-Markovian nature of social contagions, many non-Markovian models with memory characteristic have been proposed in recent years.[33,46–55] The research on social contagions with the reinforcement effect based on non-redundant information memory is receiving extensive attention from researchers. Based on the fact that the amount of information that an individual can provide is finite, the non-redundant information transmission method that only allows once successful information transmission between a pair of individuals is adopted. Each individual can remember the non-redundant behavior information passed to him/her by all his/her neighbors.[46] To avoid risks, the probability of behavior adoption when the behavior information is received again depends on the number of previously received behavior information, and before the adoption threshold is exceeded, the more the same behavior information received before, the greater the probability of adopting the behavior.[56]

In numerous literature, the adoption threshold of individuals is usually set to the same static threshold. However, heterogeneity is a topic of great interest for reflecting the ubiquitous inter-individual differences in real social systems.[47,52–55,57,58] In some binary propagation threshold models, the adoption threshold in the population has two static values: equal to 1 and greater than 1, reflecting the high

†Corresponding author. E-mail: wwzqbc@cqmu.edu.cn; wwzqbx@hotmail.com
© 2022 Chinese Physical Society and IOP Publishing Ltd

and low willingness to adopt the behavior.[47,52] Furthermore, some researchers set the adoption threshold of individuals to obey a certain probability distribution, which is more appropriate and reasonable than the binary threshold model to reflect the heterogeneity of adoption thresholds. For instance, Karampourniotis *et al.*[53] observed the non-monotonic variation of cascade size by changing the standard deviation of the threshold distribution obeying a truncated normal distribution and found that there is a specific standard deviation to optimize the spreading when the initiator set is given. Peng *et al.*[54] proposed a heterogeneous propagation threshold model, in which the adoption threshold is positively correlated with degree and a parameter obeying the Gaussian distribution. It can be found that increasing the mean of the adoption threshold distribution will inhibit social contagions. In contrast, how the standard deviation of the adoption threshold distribution affects the changing trend of the outbreak threshold and phase transition is related to the mean adoption threshold and the heterogeneity of the degree distribution. The adoption thresholds of distinct real-world social systems may follow different distribution forms, which is one of the differences in social systems. In addition, in some studies, the setting that individuals can contact all their neighbors is not reasonable enough, and individuals' time, energy and other resources are often limited.[59–63] In contact-limited social contagions, limited contact ability leads to heterogeneity in the practical information transmission probability, and this heterogeneity increases with the increase of degree distribution heterogeneity. For this reason, Wang *et al.* developed a heterogeneous edge-based compartmental (HEBC) theory. They found that when the network structure heterogeneity exceeds a certain critical value, the growth pattern of the final adoption size on the information transmission probability changes from being continuous to being discontinuous as the limited contact capacity increases.[62] Furthermore, Zhu *et al.* reported that the crossover phenomenon in the growth pattern of contact-limited social contagions can arise by adequately adjusting the adoption threshold, average degree, or initial seed ratio.[63] Considering both the limited contact capacity and the adoption thresholds obeying a certain distribution, there is still a lack of research on the impact of different distribution forms of heterogeneous adoption thresholds on contact-limited social contagions.

This paper compares the time evolutions, the final behavior adoption size, the outbreak threshold, and the phase transition under the four threshold distribution forms: the Gaussian distribution, log-normal distribution, exponential distribution, and power-law distribution. Notably, the above distributions occupy an important position in both theoretical research and practical application. According to probability theory, when the adoption thresholds obey different probability distribution forms, even if the mean and standard deviation are the same, the distribution shapes of the probability density functions are also different. Through extensive numerical simulations on the Erdös–Rényi (ER) networks and the scale-free (SF) networks, we find that the spreading process of social contagions has a hierarchical characteristic. To be specific, there are three spreading stages, individuals with large degrees and small adoption thresholds adopt the behavior first, and the adoption threshold (degree) of adopted individuals in the second stage generally increases (decreases). In addition, different threshold distributions cause different spreading processes. Further, we investigate how the standard deviation of the threshold distribution affects the steady state of contact-limited social contagions on ER networks. It is shown that as the standard deviation of different threshold distributions increases, there is a change from a discontinuous first-order phase transition to a continuous second-order phase transition for some threshold distributions, and the final adoption size and outbreak threshold will change and finally tend to be stable. On the SF networks, when the adoption thresholds obey the Gaussian distribution, for the case where the standard deviation of the threshold distribution is relatively small, it is found that the behavior adoption can explode only if the degree exponent of SF networks is moderate. Similar qualitative results are also shown from theoretical predictions based on heterogeneous edge-based compartmental theory.

The rest of this paper is arranged as follows: In Section 2, we describe the dynamics of contact-limited social contagions considering heterogeneous adoption threshold. In Section 3, we develop the heterogeneous edge-based compartmental (HEBC) theory to analyze the mechanism of social contagions qualitatively. In Section 4, extensive numerical simulations and theoretical predictions are performed. In Section 5, conclusions are drawn.

2. Heterogeneous contact-limited threshold model

In the human population, there is a universally recognized fact that individuals often have limited resources (such as time and energy), and some personal characteristics of individuals are also different. The former may limit contact capacity, the latter may cause the heterogeneity of adoption thresholds, both of which will significantly affect the dynamics of social contagions. The proposed heterogeneous contact-limited threshold model is based on the generalized non-Markovian susceptible-adopted-recovered (SAR) model, and it considers both the limited contact capacity and the adoption threshold obeying a certain distribution. In the SAR model, it is specified that there are three possible states in the population according to whether the individual participates in the spreading and has adopted the

behavior, namely, susceptible state (S state), adopted state (A state), and recovered state (R state).

In the initial stage, a tiny percentage (Q_0) of individuals are randomly selected to be in A state (seeds). The remaining individuals are in S state, and these S-state individuals do not initially get any behavioral information from the seeds (i.e., $m = 0$). At each time step, each A-state individual j with degree k' attempts to transmit the behavioral information to his/her neighbors with a certain probability. If a random S-state individual i with degree k receives the information from individual j, his/her cumulative number of information m_i will increase one (i.e., $m_i = m_i + 1$), which causes the non-Markovian effects. Moreover, individual i will not receive the same behavioral information from individual j (i.e., the non-redundant information transmission). When $m_i \geq T_i$ (threshold of individual i), individual i adopts the behavior. In addition, all A-state individuals try to recover with probability γ. If all A-state individuals have become R-state individuals, the dynamics of social contagion terminates. R-state individuals refer to individuals who have adopted the behavior but do not participate in transmitting the behavioral information.

Firstly, in view of the differences in the willingness of individuals to accept the behavior, the heterogeneity of the adoption threshold is considered in the proposed heterogeneous contact-limited threshold model. Precisely, the random variable β representing the adoption threshold distribution (threshold distribution for short) and the degree k jointly determine the adoption threshold T, i.e., $T = \beta k$. In other words, in the proposed model, not all individuals have the same threshold, but each individual has its own specific threshold, which reflects the heterogeneity of individuals. An S-state individual i with degree k does not adopt the behavior unless the amount of information about the behavior it receives from different neighbors is equal to or greater than its adoption threshold (i.e., $m \geq \lceil \beta k \rceil$). In the numerical simulations, the value of β is discrete and the interval is set as $\varepsilon = 10^{-4}$. In this paper, we consider the four probability distributions of the threshold distribution β, namely Gaussian distribution, log-normal distribution, exponential distribution and power-law distribution. The basic functional forms of the four threshold distributions are as follows:

$$f(\beta) \sim \begin{cases} \frac{1}{\sqrt{2\pi}\delta} \exp\left[-\frac{(\beta-\mu)^2}{2\delta^2}\right], & \text{Gaussian,} \\ \frac{1}{\beta\sqrt{2\pi}\delta} \exp\left[-\frac{(\ln\beta-\mu)^2}{2\delta^2}\right], & \text{log normal,} \\ \exp(-\overline{\lambda}\beta), & \text{exponential,} \\ \beta^{-\alpha}, & \text{power law.} \end{cases} \tag{1}$$

Since the adoption threshold T cannot be greater than the degree k, the threshold distribution β lies in the range $0 \leq \beta \leq 1$, otherwise susceptible individuals will never adopt the behavior. In the above threshold distributions, the mean M and the standard deviation Δ are two very important parameters. Obviously, different threshold distributions have different M and Δ. For Gaussian threshold distribution, the mean $M = \mu$, and the standard deviation $\Delta = \delta$. Differently, the mean of the log-normal threshold distribution is $M = \exp(\mu + \delta^2/2)$, and its standard deviation is $\Delta = [\exp(\delta^2) - 1]\exp(2\mu + \delta^2)$. In particular, the mean and standard deviation of the exponential threshold distribution is the same, which is $M = \Delta = \overline{\lambda}$. When β possesses a power-law distribution, which is a highly skewed distribution, there is no explicit expression for the mean and standard deviation.

In addition, in contact-limited social contagions, it is not always possible for the A-state individual to select his/her every edge to transmit the behavioral information, that is, the number of accessible edges of the A-state individual is limited. Therefore, combined with the above threshold heterogeneity, a heterogeneous contact-limited threshold model is proposed in this paper. In contact-limited propagation, an A-state individual j with degree k' that has adopted the behavior will randomly choose $H(k')$ edges from all its edges (i.e., unpreferential contact process) to transmit the behavioral information to its adjacent individuals, where $H(k')$ represents the contact capacity of individual j and the actual value of $H(k')$ does not exceed k'. In other words, the probability that each edge of individual j is selected is $H(k')/k'$. The information transmission probability (transmission probability for short) of the selected edge is λ, and the effective information transmission probability can be obtained as $\lambda H(k')/k'$. Fixed the degree distribution $p(k)$ and the mean M and standard deviation Δ of the threshold distribution, then we can compare and analyze the impact of different forms of threshold distribution on contact-limited social contagions.

3. Theoretical analysis

In the proposed model, the dynamical heterogeneity of the contagion system is mainly reflected in two aspects. Firstly, an individual's adoption threshold depends on its degree and other personal characteristics. Thus the adoption threshold usually varies from individual to individual. Secondly, considering that the contact ability of A-state individuals is restricted, the A-state neighbors connected to different edges of S-state individuals may have different degrees, which leads to the heterogeneity of the effective transmission probability of the edges. Note that the two kinds of dynamical heterogeneity are closely related to the network structure heterogeneity. Given the above-mentioned dynamical heterogeneity and the dynamical correlations caused by social reinforcement, here our goal is to describe the contact-limited social contagions with heterogeneous adoption thresholds through HEBC theory.

For a random individual i with degree k, its k neighbor individuals usually have different degrees. We denote $\pi_{k'}(t)$ as the probability that a neighbor j with degree k' has not transmitted the information to individual i along the edges between it and i until time t. Considering all possible values of degree k', the probability that individual i has not received an information until time t is

$$\pi(t) = \frac{1}{\langle k \rangle} \sum_{k'=0} k' p(k') \pi_{k'}(t), \tag{2}$$

where $\langle k \rangle$ is the average degree, and $k'p(k')/\langle k \rangle$ is the probability that individual i have neighbors with degree k'. The probability that individual i receives m pieces of non-redundant information by time t is

$$\omega(k, m, \pi(t)) = (1 - Q_0) C_k^m \pi(t)^{k-m} [1 - \pi(t)]^m, \tag{3}$$

where $1 - Q_0$ represents only individuals who are initially in the S state can receive information from their neighbors.

Individual i will not adopt the behavior unless the amount m of information it receives is not less than its adoption threshold βk, where the adoption threshold distribution β takes a certain value β_i with probability $f(\beta_i)$. Considering all possible values of β, the probability that individual i is susceptible by time t is

$$s(k, \pi(t)) = \sum_{\beta} f(\beta) \sum_{m=0}^{\lceil \beta k \rceil - 1} \omega(k, m, \pi(t)). \tag{4}$$

Considering all possible values of degree k, we can get the proportion of susceptible individuals at time t as

$$S(t) = \sum_{k} p(k) s(k, \pi(t)). \tag{5}$$

Based on the definition of $\pi_{k'}(t)$ given above, it can be further divided into

$$\pi_{k'}(t) = \tau_{k'}^S(t) + \tau_{k'}^A(t) + \tau_{k'}^R(t), \tag{6}$$

where $\tau_{k'}^S(t)$, $\tau_{k'}^A(t)$ and $\tau_{k'}^R(t)$, respectively, represent the probability that individual j with degree k' is susceptible, adopted and recovered and has not passed information to his/her neighbors until time t.

Assume that individual i is in the cavity state,[64,65] that is, individual i can receive information from his/her neighbors while cannot transmit information to them. Therefore, one of its initial susceptible neighbors, j, whose degree is k', cannot receive information from i but can receive information from the other $k' - 1$ neighbors. Similar to Eq. (3), the probability that individual j receives m pieces of information by time t is

$$\psi(k', m, \pi(t)) = (1 - Q_0) C_{k'-1}^m \pi(t)^{k'-m-1} [1 - \pi(t)]^m. \tag{7}$$

For a given threshold distribution function $f(\beta)$, the following two kinds of individuals may exist in the network: (i) activists with adoption threshold $T_k = \lceil \beta k \rceil \leq 1$; (ii) bigots with adoption threshold $T_k > 1$. More specifically, for individual j with degree k', the probability of being an activist is

$$G(k') = \sum_{\beta=0}^{1/k'} f(\beta), \tag{8}$$

and the probability of being a bigot is $1 - G(k')$. From Eq. (8), it can be seen that the distribution form of β will affect the probability that individual j is an activist. Then, we can obtain the probability that individual j is susceptible at time t is

$$\begin{aligned} \tau_{k'}^S(t) \;=\; & G(k') \pi(t)^{k'-1} \\ & + \sum_{\beta=1/k'+\varepsilon} f(\beta) \sum_{m=0}^{\lceil \beta k' \rceil - 1} \psi(k', m, \pi(t)). \end{aligned} \tag{9}$$

A random A-state individual j whose degree is k' has contact capacity $H(k')$ and the process of its selecting neighbors is random, thus for each edge of j, the probability of being selected is $H(k')/k'$, and the effective information transmission probability is $\lambda H(k')/k'$. When any A-state individual j transmits the information to his/her S-state neighbors, $\pi_{k'}(t)$ will decrease. Hence, we can get the evolution of $\pi_{k'}(t)$ as

$$\frac{\mathrm{d}\pi_{k'}(t)}{\mathrm{d}t} = -\frac{\lambda H(k')}{k'} \tau_{k'}^A(t). \tag{10}$$

Here, $\tau_{k'}^R(t)$ will increase only when both conditions are satisfied: (i) A-state individual j with degree k' does not transmit information to individual i with probability $1 - \frac{\lambda H(k')}{k'}$; (ii) individual j recover with probability γ. Therefore, the evolution of $\tau_{k'}^R(t)$ is

$$\frac{\mathrm{d}\tau_{k'}^R(t)}{\mathrm{d}t} = \gamma \left[1 - \frac{\lambda H(k')}{k'} \right] \tau_{k'}^A(t). \tag{11}$$

Combining Eqs. (10) and (11) and the initial conditions [i.e., $\pi_{k'}(0) = 1$ and $\tau_{k'}^R(0) = 0$], we have

$$\tau_{k'}^R(t) = \gamma \left[\frac{k'}{\lambda H(k')} - 1 \right] [1 - \pi_{k'}(t)]. \tag{12}$$

Substituting Eqs. (9) and (12) into Eq. (6), we can reach the expression of $\tau_{k'}^A(t)$. Then, substituting the expression of $\tau_{k'}^A(t)$ into Eq. (10), we can rewrite Eq. (10) as

$$\begin{aligned} \frac{\mathrm{d}\pi_{k'}(t)}{\mathrm{d}t} \;=\; & g[\pi_{k'}(t)] = -\frac{\lambda H(k')}{k'} \Bigg\{ \pi_{k'}(t) - \Bigg[G(k') \pi(t)^{k'-1} \\ & + \sum_{\beta=1/k'+\varepsilon} f(\beta) \sum_{m=0}^{\lceil \beta k' \rceil - 1} \psi(k', m, \pi(t)) \Bigg] \Bigg\} \\ & + \gamma \left[1 - \frac{\lambda H(k')}{k'} \right] [1 - \pi_{k'}(t)]. \end{aligned} \tag{13}$$

Let $S(t)$, $A(t)$ and $R(t)$ denote the proportions of individuals who are susceptible, adopted and recovered at time t, respectively. When the social contagion ceases, there are only S-state individuals and R-state individuals in the system, and

$R(\infty)$ represents the final adoption size. We can also give the evolution equations of $A(t)$ and $R(t)$ according to the model description in Section 2,

$$\frac{\mathrm{d}A(t)}{\mathrm{d}t} = -\frac{\mathrm{d}S(t)}{\mathrm{d}t} - \gamma A(t), \tag{14}$$

$$\frac{\mathrm{d}R(t)}{\mathrm{d}t} = \gamma A(t). \tag{15}$$

Based on Eqs. (2)–(5) and (14)–(15), we can provide a general description of contact-limited social contagions with heterogeneous adoption thresholds.

When $t \to \infty$, the dynamics of social contagions reaches a steady state, all individuals no longer change their states, that is, $\mathrm{d}\pi_{k'}(\infty)/\mathrm{d}t = 0$. Therefore, we have

$$\pi_{k'} = G(k')\pi^{k'-1} + \sum_{\beta=1/k'+\varepsilon} f(\beta) \sum_{m=0}^{\lceil \beta k' \rceil - 1} \psi(k', m, \pi) + \gamma\left[\frac{k'}{\lambda H(k')} - 1\right][1-\pi_{k'}], \tag{16}$$

where $\pi_{k'}$ represents $\pi_{k'}(\infty)$ and π represents $\pi(\infty)$, and the same in the following. By numerically iterating Eqs. (7) and (16), we can obtain the value of $\pi_{k'}$. Then, by utilizing Eqs. (2)–(5), the values of $S(\infty)$ and $R(\infty) = 1 - S(\infty)$ can be obtained.

In addition to $R(\infty)$, the outbreak threshold λ_{c} (i.e., the critical information transmission probability) is also an essential measure of the steady-state of propagation. However, the nonlinearity of Eqs. (7) and (16) makes it impossible to obtain an explicit analytical solution of λ_{c}. In general, the linear stability analysis method is used to describe the system dynamics near the critical point. Assume that the n degrees of the social system are k'_1, k'_2, …, k'_n, individuals with the same degree k'_l are assigned a variable $\pi_{k'_l}$ $(l = 1, 2, \ldots, n)$, that is, the social system is described by n variables. According to the linear stability analysis method, in the system with n variables described by Eq. (13), these n variables remain unchanged at the critical point $(\pi_{k_1^\star}, \pi_{k_2^\star}, \ldots, \pi_{k_n^\star})$, thus we have $g[\pi_{k_l^\star}] = 0$ $(l = 1, 2, \ldots, n)$. The point near the critical point can be expressed as $\pi_{k'_1} = \pi_{k_1^\star} + \nu_1$, $\pi_{k'_2} = \pi_{k_2^\star} + \nu_2$, …, $\pi_{k'_n} = \pi_{k_n^\star} + \nu_n$, where ν_1, ν_2, …, ν_n are all small quantities. Considering n variables $\pi_{k'_1}$, $\pi_{k'_2}$, …, $\pi_{k'_n}$, performing Taylor expansion on the right-hand side of Eq. (13) at the critical point $(\pi_{k_1^\star}, \pi_{k_2^\star}, \ldots, \pi_{k_n^\star})$, and ignoring the second-order terms and smaller higher-order infinitesimals, we obtain

$$\frac{\mathrm{d}\boldsymbol{\nu}}{\mathrm{d}t} = \boldsymbol{J}\boldsymbol{\nu}, \tag{17}$$

where $\boldsymbol{\nu}$ is an n-element vector $(\nu_1, \nu_2, \ldots, \nu_n)$, $\boldsymbol{J}$ is a Jacobian matrix,

$$\boldsymbol{J} = \begin{pmatrix} \frac{\partial g}{\partial \pi_{k'_1}} & \frac{\partial g}{\partial \pi_{k'_2}} & \cdots & \frac{\partial g}{\partial \pi_{k'_n}} \\ \frac{\partial g}{\partial \pi_{k'_1}} & \frac{\partial g}{\partial \pi_{k'_2}} & \cdots & \frac{\partial g}{\partial \pi_{k'_n}} \\ \vdots & \vdots & \ddots & \vdots \\ \frac{\partial g}{\partial \pi_{k'_1}} & \frac{\partial g}{\partial \pi_{k'_2}} & \cdots & \frac{\partial g}{\partial \pi_{k'_n}} \end{pmatrix},$$

where all derivatives take the value at the critical point.

4. Simulation and analysis

In this section, we study the impact of the distribution of heterogeneous adoption thresholds on contact-limited social contagions through the results of theoretical predictions and numerical simulations on the two network model: (i) the ER model;[66] (ii) the SF model[67] with degree distribution $p(k) \sim k^{-\gamma_{\mathrm{D}}} (3 \le k \le \sqrt{N})$, where the degree distribution heterogeneity is negatively related to the degree exponent γ_{D}. Figures 1–5 show the theoretical or simulated results on the ER networks, and Fig. 6 presents the theoretical results on the SF networks. There are 10^3 independent simulations on a fixed network, performed to obtain the corresponding average results. There is no degree-degree correlations when the network size N is large enough. We set the network size, average degree, recovery probability, contact ability and initial seed density as $N = 10^4$, $\langle k \rangle = 10$, $\gamma = 1.0$, $H(k) = c = 8$ and $Q_0 = 0.0005$, respectively.

First, we study the hierarchical phenomena of the spreading process of contact-limited social contagions. The so-called hierarchical nature of the spreading process is that some individuals adopt the behavior first, and some individuals adopt the behavior later. Figure 1 shows the time evolutions of contact-limited social contagions with adoption thresholds obeying a Gaussian distribution. The total number of time steps t_{all} (convergence time) at the end of the spreading reflects the spreading efficiency. Specifically, the larger the t_{all} is, the weaker the spreading efficiency is. In order to measure the diversity of the attribute χ of newly adopted individuals, the inverse participation ratio $D_\chi(t)$[68] is used as the diversity measure, which is defined as

$$D_\chi(t) = \frac{1}{\sum_\chi \left[\frac{\xi_\chi(t) - \xi_\chi(t-1)}{\xi(t) - \xi(t-1)}\right]^2}, \tag{18}$$

where the attribute $\chi \in \{k, T, \beta\}$ with k, T and β representing the degree, adoption threshold and threshold distribution, respectively, and $\xi(t)$ $(\xi_\chi(t))$ is the number of A-state individuals (A-state individuals with attribute χ) at time t. The larger the $D_\chi(t)$, the larger the number of distinct communities divided according to the value of attribute χ. In particular, $D_\chi(t) = 1$ indicates that the newly A-state individuals have the same attribute χ.

As shown in Fig. 1, the three regions (regions I, II and III) divided by three different colors represent the three stages of the spreading process. The time step at which $n_A(t)$ and $\langle T_A(t)\rangle$ reach the peak value is the basis of dividing the propagation stage. In the I stage, $n_A(t)$ increases with time t and reaches the peak (when $t = 11$), the value of $\langle k_A(t)\rangle$ is large (around 10) and changes little with time t, the value of $\langle T_A(t)\rangle$ ($\langle \beta_A(t)\rangle$) increases with time t and is less than 1 (less than 0.1). In the II stage, $n_A(t)$ decreases to a minimum value as time t increases, and the value of $\langle T_A(t)\rangle$ ($\langle \beta_A(t)\rangle$) increases to a peak value (big value) as time t increases, and the value of $\langle k_A(t)\rangle$ decreases compared with that of the I stage. In addition, the values of $D_k(t)$, $D_T(t)$ and $D_\beta(t)$ increase to a peak value and then decrease in the II stage. In the III stage, the value of $n_A(t)$ is minimal, and the value of $\langle k_A(t)\rangle$ continues to decrease compared with that of the II stage, $\langle \beta_A(t)\rangle$ continues to increase with time t, and the value of $\langle T_A(t)\rangle$ slightly decreases compared with the peak value.

The newly A-state individuals of the three stages have a big difference in the degree and adoption threshold, reflecting the hierarchical characteristics of the social contagion process with unbiased contacts. In general, in the I stage, many individuals with high degrees and small adoption thresholds adopt the behavior first. In the II stage, compared with the I stage, some individuals with more minor degrees (large in fact) and relatively large adoption thresholds adopt the behavior. Finally, in the III stage, a few individuals with large degrees and large adoption thresholds ($\langle k_A(t)\rangle$ is about 6, $\langle T_A(t)\rangle$ is about 1.5) adopt the behavior. In this way, the behavior is progressively spread over the network.

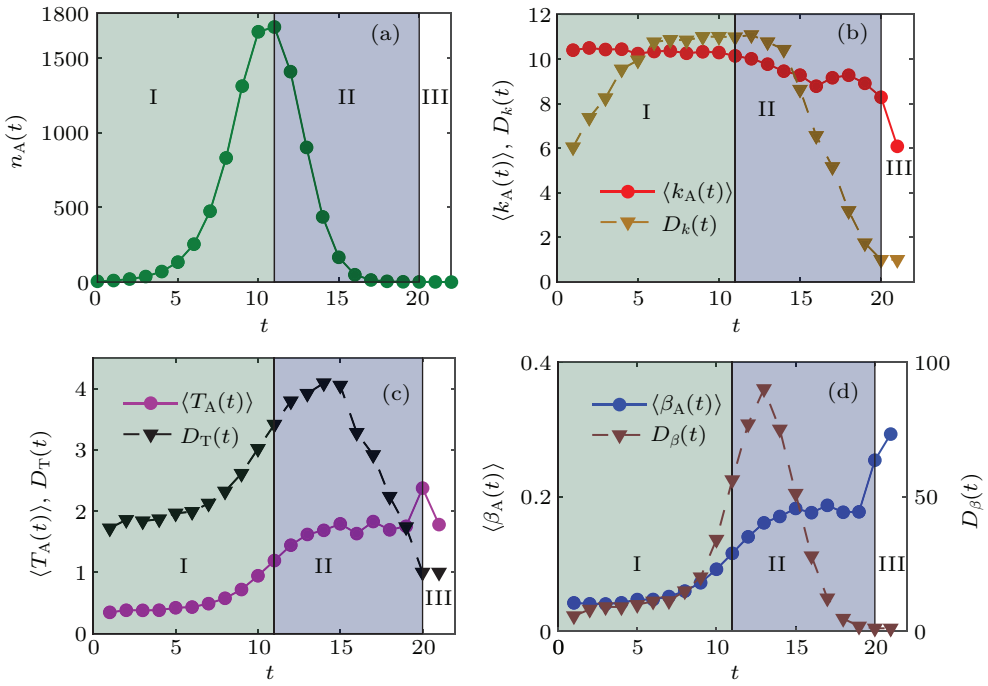


Fig. 1. For Gaussian threshold distribution, the time evolutions of contact-limited social contagions on the ER networks. (a) The number $n_A(t)$, (b) average degree $\langle k_A(t)\rangle$, degree diversity $D_k(t)$, (c) average adoption threshold $\langle T_A(t)\rangle$, adoption threshold diversity $D_T(t)$, (d) average threshold distribution $\langle \beta_A(t)\rangle$ and threshold distribution diversity $D_\beta(t)$ of newly A-state individuals versus time steps t. Other parameters are set as $M = 0.1$, $\Delta = 0.1$ and $\lambda = 0.6$.

Next, we study how different threshold distribution forms affect the hierarchy of the spreading process. Figure 2 shows the time evolutions of contact-limited social contagions under four different threshold distribution forms (Gaussian distribution, log-normal distribution, exponential distribution, and power-law distribution). From Fig. 2, we see that the spreading efficiency under the Gaussian threshold distribution is weakest (i.e., t_{all} is largest), and the propagation efficiency under the other three threshold distributions is relatively strong, among which the propagation efficiency under the power-law threshold distribution is the strongest. For the propagation rate, as shown in Fig. 2(a), the spreading rate under the power-law threshold distribution is faster (i.e., $n_A(t)$ is larger (smaller) when t is small (large)), the slowest is under the Gaussian distribution, and the spreading rate under log-normal distribution and exponential distribution is very close. As shown in Figs. 2(b), 2(c) and 2(d), in the I and II stage, the $\langle k_A(t)\rangle$, $\langle T_A(t)\rangle$ and $\langle \beta_A(t)\rangle$ under these four threshold distributions are all close, $\langle k_A(t)\rangle$ decreases slightly around $\langle k\rangle = 10$ and $\langle T_A(t)\rangle$ ($\langle \beta_A(t)\rangle$) increases from a value less than 0.1 (1) to about 0.2 (2). While in the III stage, the $\langle k_A(t)\rangle$ under the exponential threshold distribution increases with t to a relatively large value (close to 14), and the $\langle \beta_A(t)\rangle$ under log-normal distribution and power law distribution decreases with t to a smaller value. Contrastively, when β obeys exponential distribution and Gaussian distribution, $\langle \beta_A(t)\rangle$ increases with

t to a larger value (about 0.28). In addition, for any threshold distribution here, $D_k(t)$ and $D_\beta(t)$ increase to a relatively large value as t increases in stage I, because the number of newly A-state individuals $n_A(t)$ increases with t in stage I, while in the vicinity of stage II and stage III, $D_k(t)$ and $D_\beta(t)$ decrease to a relatively small value as t increases [see Figs. 2(e), 2(f), and 2(g)].

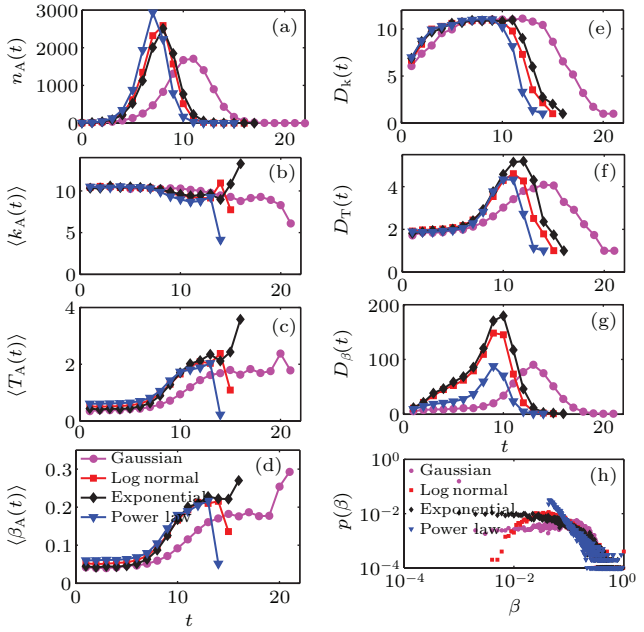


Fig. 2. Effects of threshold distribution forms on the hierarchy of the spreading process of contact-limited social contagions on the ER networks. (a) The number $n_A(t)$, (b) mean degree $\langle k_A(t)\rangle$, (c) average adoption threshold $\langle T_A(t)\rangle$, (d) average threshold distribution $\langle \beta_A(t)\rangle$, (e) degree diversity $D_k(t)$, (f) adoption threshold diversity $D_T(t)$ and (g) threshold distribution diversity $D_\beta(t)$ of newly A-state individuals versus time t for the Gaussian threshold distribution (purple circles), log-normal threshold distribution (red squares), exponential threshold distribution (black diamonds) and power law threshold distribution (blue down triangles). (h) The probability distribution diagram of threshold β under the four threshold distribution forms. Other parameters are set as $M = 0.1$, $\Delta = 0.1$, and $\lambda = 0.6$.

In brief, when the network and the mean and standard deviation of the threshold distribution are fixed, the probability distribution of β is very different under different distributions. As shown in Fig. 2(h), when the threshold distribution β obeys the Gaussian distribution, the threshold distribution is relatively uniform; when β obeys the power-law distribution, there is almost no small β, and the probability that β is between 0.1 and 1 is large. For the case that β obeys the exponential distribution, the probability that β is very small (between 0.001 and 0.01) is greater than the other three distributions. For the probability that $\beta < 0.01$, the exponential distribution > log-normal distribution. For the probability that β is between 0.01 and 0.1, the log-normal distribution > exponential distribution. It is known that $T = \beta k$, so the distribution of adoption threshold T is also very different, which leads to the difference in the spreading process under different threshold distributions. In addition, when β obeys the exponential distribution, the individuals with the largest thresholds and degrees adopt the behavior in stage III, and when β obeys the power-law distribution, the individuals with the most minor thresholds and degrees adopt the behavior in stage III.

Further, it is necessary to study the effects of the threshold distribution form on the final behavior adoption size $R(\infty)$ and outbreak threshold λ_c (the critical information transmission probability) of contact-limited social contagions. According to Ref. [54], the influence of the standard deviation of the threshold distribution on social contagions depends on the size of the mean of the threshold distribution. Specifically, for some relatively large threshold distribution mean, the changes of the phase transition and outbreak threshold of the propagation system are more abundant. Therefore, in this article, we set the mean threshold distribution to be a relatively large value (i.e., $M = 0.15$) and observe the spreading results under different threshold distribution and standard deviations. From Fig. 3, we can see that the theoretical predictions and simulation results of $R(\infty)$ under the power-law threshold distribution are slightly biased when $\Delta = 0.1$ [see Fig. 3(a)], and the consistency between them is relatively good in Figs. 3(b) and 3(c). In addition, the peak value of of the relative variance V_R of the simulated $R(\infty)$ can be used to estimate the simulated value of λ_c [69] [see Figs. 3(d)–3(f)]. V_R is defined as

$$V_R = \frac{\langle R(\infty) - \langle R(\infty)\rangle\rangle^2}{\langle R(\infty)\rangle^2}, \tag{19}$$

where $\langle\cdots\rangle$ denotes ensemble averaging, and 10^3 independent dynamical realizations in a fixed network are performed to obtain V_R.

For $\Delta = 0.1$, the inset of Fig. 3(a) shows that the probability distribution under the Gaussian or log-normal threshold distribution has prominent fat tails (i.e., the probability that $\beta > 0.1$ is relatively large), and there are also quite a few individuals with $\beta \leq 0.1$. In contrast, the β of almost all individuals is roughly greater than or equal to 0.1 when β obeys a power-law distribution. For the former, when λ increases to λ_c, the individuals with $\beta \leq 0.1$ adopt the behavior almost simultaneously, making the growth form of $R(\infty)$–λ show a first-order phase transition. Then, as λ continues to increase, the individuals with $\beta > 0.1$ also adopt the behavior successively, and the system presents a second-order phase transition. For the latter, only when λ increases to λ_c, these individuals with large β will adopt the behavior in cascade, and the system presents a first-order phase transition. As the standard deviation Δ increases to 0.15 or 0.2 [see Fig. 3(b) or Fig. 3(c)], we find that the system exhibits a continuous second-order transition under different threshold distributions, which is because the probability distribution of β becomes more and more polarized with the increase of Δ. The number of individuals with a particularly small β and the number of individuals with a particularly large β both increase. In addition, as Δ increases, the relationship between the λ_c and $R(\infty)$

of different threshold distributions also changes. Obviously, as λ increases, for the power-law threshold distribution, the λ_c changes from the largest to the smallest, and when $\lambda = 1$, $R(\infty)$ is smaller than 1 more obviously, and the λ_c under the Gaussian threshold distribution is always larger than the λ_c under the log-normal threshold distribution. We can explain the phenomena mentioned above as follows: Firstly, when the mean and standard deviation of the threshold distribution is the same, the probability that β is particularly small (i.e., $\beta < 0.1$) is different for different threshold distribution forms. Individuals with very small β can quickly adopt the behavior to promote social contagions (i.e., λ_c decreases). Therefore, as the standard deviation Δ increases, when the probability that β under a certain threshold distribution is very small is larger, its λ_c is smaller. In the same way, it can be stated that when $\lambda = 1$, $R(\infty)$ under the Gaussian threshold distribution is the largest. Secondly, individuals with a particularly large β (i.e., $\beta \gg 0.1$) usually have an extensive adoption threshold, and their contact capacity is limited. Therefore, when $\lambda = 1$, individuals whose β is close to 1 may not be able to adopt the behavior, which leads to $R(\infty)$ less than 1.

Next, there is another very important phenomenon that the intersection of $R(\infty)$–λ under the exponential threshold distribution and $R(\infty)$–λ under the log-normal threshold distribution when the standard deviation $\Delta = 0.15$ [see Fig. 3(b)]. We note that when λ is relatively small, the $R(\infty)$ under the exponential threshold distribution is greater than the $R(\infty)$ under the log-normal threshold distribution, the situation is opposite when λ is large. This is because, under the exponential threshold distribution, there are many individuals whose β is relatively very small, and these individuals can quickly adopt the behavior, prompting the social contagion when λ is small. However, the exponential threshold distribution has a lot of fat tails (i.e., $\beta \gg 0.1$), and the probability of β near 0.1 under the log-normal threshold distribution accounts for the majority. Its fat tails are less relative to the exponential threshold distribution [see the inset of Fig. 3(b)]. These individuals in the fat-tailed part (i.e., individuals with a particularly large β) are challenging to adopt the behavior to suppress social contagion. Compared with the log-normal threshold distribution, the exponential threshold distribution has more fat tails, so its $R(\infty)$ is smaller.

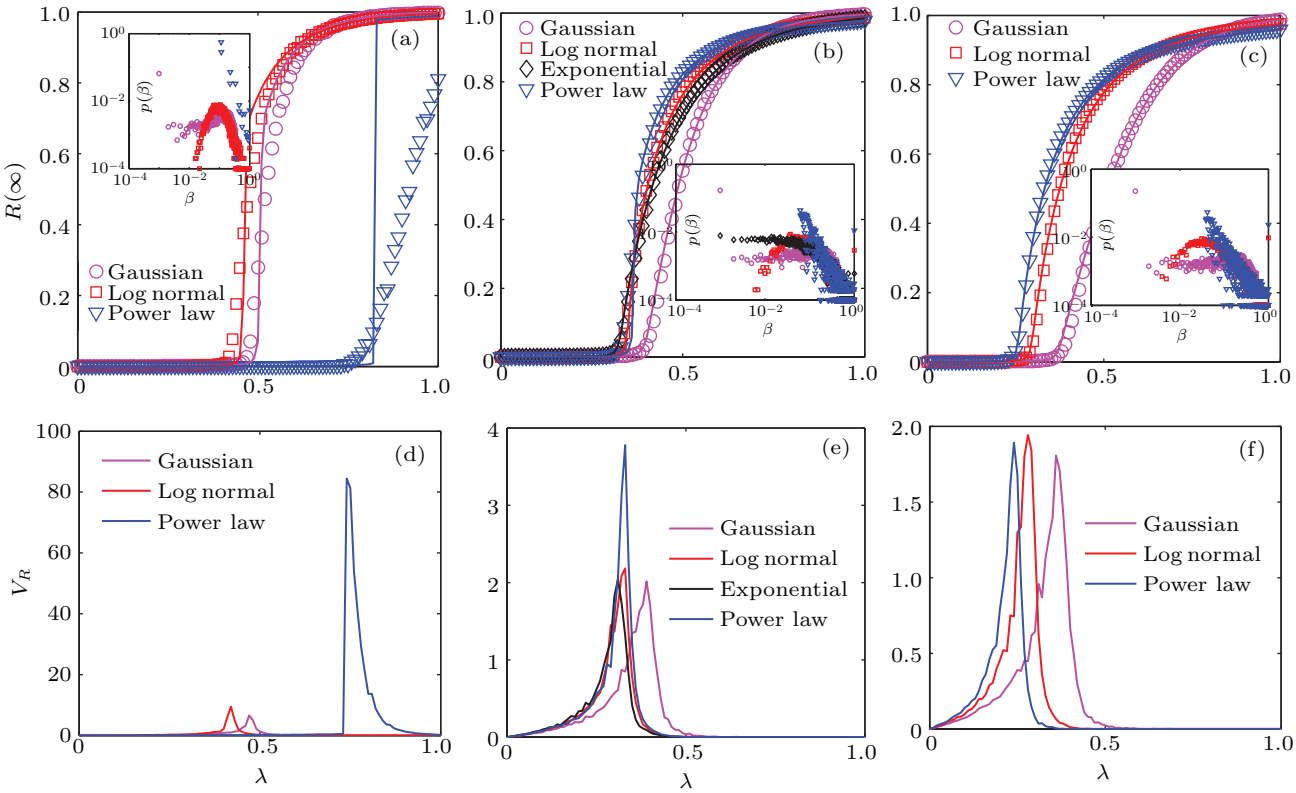


Fig. 3. The dynamics of contact-limited social contagions under different threshold forms on the ER networks. When the mean threshold distribution $M = 0.15$, the final behavior adoption size $R(\infty)$ versus the information transmission probability λ for (a) $\Delta = 0.1$, (b) $\Delta = 0.15$ and (c) $\Delta = 0.2$. The corresponding relative variance V_R versus λ for $\Delta = 0.1, 0.15, 0.2$ are presented in (d), (e) and (f), respectively. In (a), (b) and (c), different colored lines and points represent the theoretical and simulation results of $R(\infty)$ under different threshold distribution forms, respectively. The insets of (a), (b) and (c) show the corresponding probability distribution diagrams of threshold β.

It can be seen from Fig. 3 that when the average threshold distribution $M = 0.15$, the impact of different threshold distribution forms on contact-limited social contagions varies with the standard deviation Δ of the threshold distribution. For the above situation, Fig. 4 shows the theoretical results of $R(\infty)$ on the panel λ–Δ in more detail. When the spreading can break out, as Δ increases, the outbreak threshold λ_c decreases rapidly first, then tends to be stable. More concretely, the sta-

ble value of λ_c under the Gaussian threshold distribution is the largest, and the stable value of λ_c under the power-law threshold distribution is the smallest. We can understand like this that when Δ is large ($\Delta > 0.3$), the number of individuals with a small adoption threshold under the power-law threshold distribution is the largest, which is very conducive to behavior adoption and leads to a relatively minimum λ_c. Similarly, the largest number of individuals with a large adoption threshold under the Gaussian threshold distribution leads to the largest λ_c. In addition, as Δ increases, the value of $R(\infty)$ under the Gaussian threshold distribution shows a clear downward trend when λ approaches 1 [see Fig. 4(a)], while for the log-normal threshold distribution and the power-law threshold distribution, when λ is close to 1, the value of $R(\infty)$ is approximately 1 [see Figs. 4(a) and 4(b)]. We can realize that when λ is close to 1, what can affect the size of $R(\infty)$ is the proportion of individuals with a substantial adoption threshold. That is to say, when adoption thresholds obey the log-normal distribution and the power-law distribution, as Δ increases, the number of individuals with a substantial adoption threshold does not change significantly, and it increases significantly under the Gaussian threshold distribution. Regarding the system phase transition, we can notice that with the increase of Δ, there will be a crossover phenomenon under these three threshold distribution forms, from a discontinuous first-order phase transition to a continuous second-order phase transition.

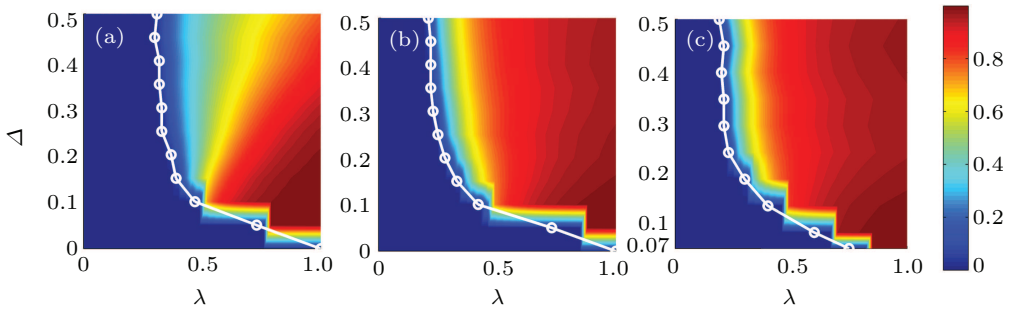


Fig. 4. On the ER networks, the final behavior adoption size $R(\infty)$ versus the information transmission probability λ and the standard deviation of threshold distributions Δ. (a) Gaussian threshold distribution, (b) log-normal threshold distribution, and (c) power law threshold distribution, showing the theoretical predictions of $R(\infty)$ in the plane λ–δ, respectively. It is noted that the results for the power low case are not shown when $\Delta < 0.07$ in (c), because the standard deviation of the power low distribution will not be equal to 0. Other parameters are the mean of threshold distributions, $M = 0.15$, $\gamma = 1.0$, $Q_0 = 0.0005$, $c = 8$.

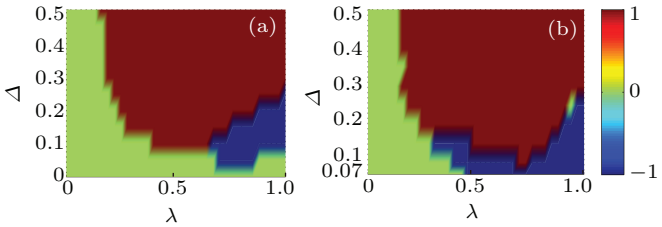


Fig. 5. On the ER networks, compared to the spreading results under Gaussian threshold distribution, the effects of log-normal threshold distribution and power law threshold distribution. In the plane λ–Δ, the color-coded values of (a) $R(\infty)$ under the log-normal threshold distribution minus $R(\infty)$ under the Gaussian threshold distribution, (b) $R(\infty)$ under the power law threshold distribution minus $R(\infty)$ under the Gaussian threshold distribution. We set 1 (red), 0 (green) and -1 (blue) to represent promoting, no affecting, and inhibiting effects, respectively. Other parameters are the mean of threshold distributions, $M = 0.15$, $\gamma = 1.0$, $Q_0 = 0.0005$, $c = 8$.

According to Fig. 4, Fig. 5 further shows the results of subtracting the theoretical value of $R(\infty)$ under the Gaussian threshold distribution from the theoretical value of $R(\infty)$ under the other two threshold distributions, respectively, when other parameters are the same. In order to show more intuitively, 1 and -1 are respectively used to indicate the cases where the result of the subtraction is greater than 0 and less than 0. In this way, it can be seen that based on the final adoption size under the Gaussian threshold distribution, the promotion or suppression of the other two threshold distribution forms varies with the changes of Δ and λ. Compared Fig. 5 with Fig. 4, it can be observed that the green area in Fig. 5 corresponds to the local behavior adoption region in Fig. 4 (i.e., when the spreading is over, there are very few adopted individuals). Moreover, the red area and blue area in Fig. 5 correspond to the global behavior adoption region in Fig. 4 (i.e., the spreading can break out, and there is a certain percentage of adopted individuals). From the distribution characteristics of the blue area and the red area in Fig. 5, it can be found that when the average adoption threshold $M = 0.15$ and other parameters are fixed, for the log-normal threshold distribution, when the value of Δ is small, and the value of λ is large (e.g., $0.1 < \Delta < 0.2$ and $0.7 < \lambda \leq 1$), its propagation effect is not as good as the Gaussian threshold distribution [see Fig. 5(a)]; for the power-law threshold distribution, when the value of Δ is small (e.g., $0.07 < \Delta < 0.2$), it does not propagate as well as the case of the Gaussian threshold distribution [see Fig. 5(b)]. To explain the above phenomenon, the most fundamental reason is that under different standard deviations, the probability distribution diagrams of these types of threshold distributions are different. Compared with the Gaussian threshold distribution, the promotion or inhibition of the other two threshold distributions depends on the number of individuals with a relatively small adoption threshold when λ is small, and depends on the number of individuals with a relatively large adoption threshold when λ is large.

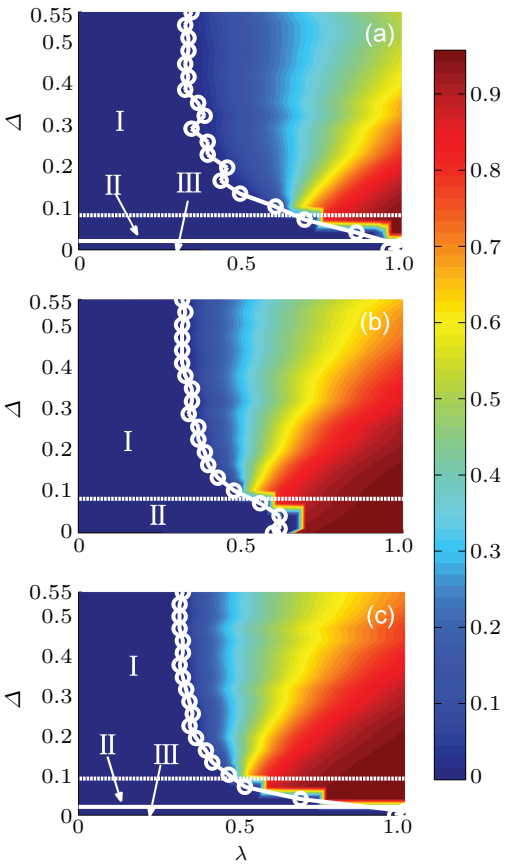


Fig. 6. On the SF networks, the final behavior adoption size $R(\infty)$ under the Gaussian threshold distribution versus λ and Δ. The color-coded values of the theoretical $R(\infty)$ in the plane λ–Δ for (a) $\gamma_D = 2.1$, (b) $\gamma_D = 3.0$ and (c) $\gamma_D = 3.5$. In region III, there is only local behavior adoption, and in region I (II), the grow pattern of the dependence of $R(\infty)$ on λ is continuous (discontinuous). The circles with straight lines in the figure represent the simulated values of the outbreak threshold λ_c. Other parameter is the mean of threshold distributions $M = 0.15$, $\gamma = 1.0$, $Q_0 = 0.0005$, $c = 8$.

Finally, on the SF networks with degree distribution $p(k) = k^{-\gamma_D}$, we also perform lots of theoretical fittings to explores the influence of the heterogeneity of degree distribution on contact-limited social contagions with Gaussian threshold distribution. Figure 6 shows the theoretical predictions of $R(\infty)$ versus Δ and λ. It is known that the degree distribution heterogeneity of the SF network decreases as the power-law degree exponent γ_D increases. According to the size of $R(\infty)$ and the type of phase transition, Fig. 6 can be divided into different regions. As shown in Fig. 6, when the heterogeneity of the degree distribution is relatively substantial [e.g., $\gamma_D = 2.1$, see Fig. 6(a)] and relatively weak [e.g., $\gamma_D = 3.5$, see Fig. 6(c)], only when the standard deviation Δ of the threshold distribution is greater than a critical point Δ_S (see the horizontal white solid line), the behavior adoption can break out. However, when the heterogeneity of the degree distribution takes an intermediate value [e.g., $\gamma_D = 3.0$, see Fig. 3(b)], there is no region III in Fig. 3(b) (i.e., global behavior adoption can occur for any value of Δ). In general, an appropriate network structure heterogeneity promotes contact-limited social contagions. As Δ increases, there is a crossover phenomenon between regions II and I: the growing pattern of $R(\infty)$ versus λ changes from being discontinuous to being continuous (see the horizontal white dashed lines in Fig. 6). For the case of $\gamma_D = 3.0$ [see Fig. 6(b)], in region II, it can be noticed that λ_c hardly changes, while in region I, λ_c decreases first and then tends to a stable value. For the case of $\gamma_D = 2.1$ or 3.5, there is only the latter kind of change mentioned above.

5. Conclusion

In summary, we have studied heterogeneous adoption thresholds on contact-limited social contagions. First, we propose a heterogeneous contact-limited threshold model to describe the dynamics of contact-limited social contagions with adoption thresholds obeying a certain distribution, in which four threshold distributions are considered, and each adopted individual can only contact a certain number of his/her neighbors at each moment. Then, we develop a heterogeneous edge-based compartmental theory to analyze the proposed model, and numerical simulations verify the correctness of the theoretical results. Through simulations on the ER networks, we find that the spreading process of social contagions can be divided into three stages, and the average degree and average adoption threshold of newly adopted individuals change with time t. Individuals with a high degree and a small adoption threshold adopt the behavior first. In addition, we find that when the mean of the adoption threshold distribution is fixed to a medium value ($M = 0.15$), as the standard deviation of the threshold distribution increases, there will be a crossover phenomenon of growth forms under some threshold distributions. Finally, the results on the SF networks show that when the adoption thresholds obey a Gaussian distribution, and the standard deviation is very small, taking a moderate value for the network structure heterogeneity is conducive to the outbreak of contact-limited social contagions. This work just provides a starting point to understand the effects of heterogeneous adoption thresholds on contact-limited social contagions, a deeper understanding of how contact-limited social contagions on real social networks are affected by heterogeneous adoption thresholds still requires further efforts to discover.

Acknowledgements

Project supported by the National Natural Science Foundation of China (Grant Nos. 62072412, 61902359, 61672467, and 61672468), the Social Development Project of Zhejiang Provincial Public Technology Research (Grant No. 2016C33168), Zhejiang Provincial Natural Science Foundation of China (Grant No. LQ19F030010), and the Opening Project of Shanghai Key Laboratory of Integrated Administration Technologies for Information Security (Grant No. AGK2018001).

References

[1] Jeong H M, Mason S P, Barabási A and Oltvai Z N 2001 *Nature* **411** 41
[2] Dunne J A, Williams R J and Martinez N D 2002 *Proc. Natl. Acad. Sci. USA* **99** 12917
[3] Motter A E, Myers S A, Anghel M and Nishikawa T 2013 *Nat. Phys.* **9** 191
[4] Faloutsos M, Faloutsos P and Faloutsos C 1999 *ACM SIGCOMM Comput. Commun. Rev.* **29** 251
[5] Ebel H, Mielsch L I and Bornholdt S 2002 *Phys. Rev. E* **66** 035103
[6] Serrano M A and Bogu ná M 2003 *Phys. Rev. E* **68** 015101
[7] Yang Y Z, Hu M and Huang T Y 2020 *Chin. Phys. B* **29** 088903
[8] Wang W, Li W Y, Lin T, Wu T, Pan L M and Liu Y B 2021 *Appl. Math. Comput.* 126793 (In Press)
[9] Pan L M, Wang W, Tian L and Lai Y C 2021 *Phys. Rev. E* **103** 012302
[10] Watts D J and Strogatz S H 1998 *Nature* **393** 440
[11] Albert R and Barabási A L 2002 *Rev. Mod. Phys.* **74** 47
[12] Newman M E J 2003 *SIAM Rev.* **45** 167
[13] Boccaletti S, Bianconi G, Criado R, del Genio C I, Gómez-Gardeñes J, Romance M, Sendiña-Nadal I, Wang Z and Zanin M 2014 *Phys. Rep.* **544** 1
[14] Hawoong Jeong R A and Barabási A 2000 *Nature* **406** 378
[15] Callaway D S, Newman M E J, Strogatz S H and Watts D J 2000 *Phys. Rev. Lett.* **85** 5468
[16] Cohen R, Erez K, ben-Avraham D and Havlin S 2000 *Phys. Rev. Lett.* **85** 4626
[17] Song C, Havlin S and Makse H A 2005 *Nature* **433** 392
[18] Arenas A, Diaz-Guilera A, Kurths J, Moreno Y and Zhou C 2008 *Phys. Rep.* **469** 93
[19] Radicchi F 2015 *Nat. Phys.* **11** 597
[20] Li D Q, Fu B W, Wang Y P, Lu G Q, Berezin Y, Stanley H E and Havlin S 2015 *Proc. Natl. Acad. Sci. USA* **112** 669
[21] Zhang M, Wang X J, Jin L, Song M and Liao Z H 2020 *Chin. Phys. B* **29** 096401
[22] Liu J 2021 *Chin. Phys. B* **30** 016401
[23] Li W Y, Xue X, Pan L M, Lin T and Wang W 2022 *Appl. Math. Comput.* **412** 126595
[24] Saumell-Mendiola A, Serrano M A and Boguná M 2012 *Phys. Rev. E* **86** 026106
[25] Sun Y, Liu C, Zhang C X and Zhang Z K 2014 *Phys. Lett. A* **378** 635
[26] Gosak M, Duh M, Markovi R and Perc M 2021 *New J. Phys.* **23** 043039
[27] Brett T, Loukas G, Moreno Y and Perra N 2019 *Phys. Rev. E* **99** 050303
[28] Okamoto T and Ishida Y 2002 *Syst. Comput. Jpn.* **33** 81
[29] Feng Y, Ding L, Huang Y H and Guan Z H 2016 *Chin. Phys. B* **25** 128903
[30] Lu Y L, Jiang G P and Song Y R 2012 *Chin. Phys. B* **21** 100207
[31] Zan Y 2018 *Chaos, Solitons & Fractals* **110** 191
[32] Cheng Y, Huo L and Zhao L 2021 *Inf. Sci.* **564** 237
[33] Liu W, Wu X, Yang W, Zhu X and Zhong S 2019 *Appl. Math. Comput.* **343** 214
[34] Chen N, Zhu X and Chen Y 2019 *Physica A* **523** 671
[35] Zhang Y, Su Y, Li W and Liu H 2019 *Chaos, Solitons & Fractals* **121** 168
[36] Gao X and Tian L 2019 *Physica A* **514** 226
[37] Karsai M, Iniguez G, Kaski K and Kertesz J 2014 *J. R. Soc. Interface* **11** 20140694
[38] Ma Y, Xue X, Cai M and Wang W 2020 *Chin. Phys. B* **29** 128902
[39] Zhan X X, Liu C, Zhou G, Zhang Z K, Sun G Q, Zhu J and Jin Z 2018 *Appl. Math. Comput.* **332** 437
[40] Guo H, Wang Z, Sun S and Xia C 2021 *Phys. Lett. A* **398** 127282
[41] Zhu L, Liu W and Zhang Z 2021 *Math. Comput. Simul.* **188** 268
[42] Wang W, Liu Q H, Liang J, Hu Y and Zhou T 2019 *Phys. Rep.* **820** 1
[43] Peng X L and Zhang Y D 2021 *Chin. Phys. B* **30** 058901
[44] Granovetter M S 1973 *Am. J. Sociol.* **78** 1360
[45] Watts D J 2002 *Proc. Natl. Acad. Sci. USA* **99** 5766
[46] Wang W, Tang M, Zhang H F and Lai Y C 2015 *Phys. Rev. E* **92** 012820
[47] Wang W, Tang M, Shu P and Wang Z 2016 *New J. Phys.* **18** 013029
[48] Wang X, Lan Y and Xiao J 2019 *Physica A* **531** 121721
[49] Backlund V P, Saramaki J and Pan R K 2014 *Phys. Rev. E* **89** 062815
[50] Unicomb S, I niguez G and Karsai M 2018 *Sci. Rep.* **8** 3094
[51] Han L L, Lin Z H, Tang M, Zhou J, Zou Y and Guan S G 2020 *Phys. Rev. E* **101** 042308
[52] Zhu X, Tian H, Chen X, Wang W and Cai S 2018 *New J. Phys.* **20** 125002
[53] Karampourniotis P D, Sameet S, Szymanski B K, Gyorgy K and Adriana B L 2015 *PLoS One* **10** e0143020
[54] Peng H, Peng W X, Zhao D D and Wang W 2020 *Appl. Math. Comput.* **386** 125504
[55] Ren J, Yang Q, Zhu Y, Zhu X and Cai S 2020 *IEEE Acc.* **8** 61905
[56] Bao P, Shen H W and Cheng X Q 2013 *PlOS one* **8** e76027
[57] Yang Z, Cui A X and Zhou T 2011 *Physica A* **390** 4543
[58] Chatterjee S and Durrett R 2009 *Ann. Probab.* **37** 2332
[59] Xiong F, Zheng Y, Wang H, Wang X and Chen H 2021 *Future Generation Computer Systems* **114** 307
[60] Jiang J and Zhou T 2018 *Physica A* **508** 414
[61] Tian G and Wang Z C 2020 *Appl. Math. Lett.* **102** 106121
[62] Wang W, Shu P P, Zhu Y X, Tang M and Zhang Y C 2015 *Chaos* **25** 103102
[63] Zhu Y X, Cao Y Y, Chen T, Qiu X Y, Wang W and Hou R 2018 *Chaos Solitons & Fractals* **114** 408
[64] Karrer B and Newman M E J 2010 *Phys. Rev. E* **82** 016101
[65] Karrer B, Newman M E J and Zdeborová L 2014 *Phys. Rev. Lett.* **113** 208702
[66] Erdös P and Rényi A 1959 *Publ. Math. Debrecen* **6** 290
[67] Catanzaro M, Bogu ná M and Pastor-Satorras R 2005 *Phys. Rev. E* **71** 027103
[68] Lou J 2007 *Ecology* **88** 2427
[69] Chen W, Schroder M, D'Souza R M, Sornette D and Nagler J 2014 *Phys. Rev. Lett.* **112** 155701